Advances in Nano Research, *Vol. 17, No.3 (2024) 235-248*
https://doi.org/10.12989/anr.2024.17.3.235

Wave propagation in FG polymer composite nanoplates embedded in variable elastic medium

Ahmed Kadiri[1], Mohamed Bendaida[*2], Amina Attia[3], Mohammed Balubaid[4], S. R. Mahmoud[5], Abdelmoumen Anis Bousahla[2], Abdeldjebbar Tounsi[6, 7], Fouad Bourada[7] and Abdelouahed Tounsi[**7, 8]

[1]*Faculty of Technology, Department of Basic Teaching in Science and Technology, University of Sidi Bel Abbes, Algeria*
[2]*Laboratoire de Modélisation et Simulation Multi-échelle, Université de Sidi Bel Abbés, Algeria*
[3]*Engineering and Sustainable Development Laboratory, Faculty of Science and Technology, Civil Engineering Department, University of Ain Temouchent, Algeria*
[4]*Department of Industrial Engineering, King Abdulaziz University, Jeddah, Saudi Arabia*
[5]*GRC Department, Applied College, King Abdulaziz University. Jeddah 21589, Saudi Arabia*
[6]*Mechanical Engineering Department, Faculty of Science & Technology, University of Relizane, Algeria*
[7]*Material and Hydrology Laboratory, Faculty of Technology, Civil Engineering Department, University of Sidi Bel Abbes, Algeria*
[8]*Department of Civil and Environmental Engineering, King Fahd University of Petroleum & Minerals, 31261 Dhahran, Eastern Province, Saudi Arabia*

(*Received May 25, 2024, Revised August 25, 2024, Accepted August 28, 2024*)

Abstract. This study explores the transmission of waves through polymer composite nanoplates situated on varying elastic foundations. The reinforcement of these nanoplates is assured by graphene nanoplatelets (GNP). Furthermore, the material's behavior is assessed using the Halpin-Tsai model, while the precise representations of stress and strain effects are ensured by the four variables higher order shear deformation theory. The equations of motion are obtained and resolved through the application of Hamilton's principle and the trial function. The study examines how different factors, like the nonlocal parameter, strain gradient parameter, weight fraction, and variable elastic foundations affect the outcomes of wave propagation in nanoplates. This thorough investigation offers valuable insights into the difficult behavior of wave dynamics in nanoplates, this has led to substantial advancements in engineering applications for the future.
Keywords: polymer composite; wave propagation; graphene nanoplatelet; variable foundation

1. Introduction

Graphene has vast potential across micro-nano processing, energy, and healthcare sectors. It is a revolutionary material due to its remarkable mechanical and thermal properties. Buckling/bending/ vibration (Song *et al*. 2018, Sahmani *et al*. 2018, Jiao and Alavi 2018, Arefi *et al*. 2019, Kiani 2019, Aditya *et al*. 2019, Yang *et al*. 2020, Yaghoobi and Taheri 2020, Liu *et al*. 2020, Tran *et al*. 2020, Al-Furjan *et al*. 2021, Yang *et al*. 2021, Wang *et al*. 2023) of structures reinforced with graphene nanoplatelets (GNPs) and graphene platelets (GPLs) are investigated by some researchers but the Researches on examining the characteristics of wave propagation in macro, micro, and nano structures remain limited specially those reinforced by GPNs/GPLs. Hua *et al*. (2022) investigated the wave propagation behavior of sandwich plates with graphite particles filled viscoelastic material core under the hygrothermal environments. Hua *et al*. (2022) examined wave dispersion characteristics of laminated composite shells resting on viscoelastic foundations in thermal environments. Hua *et al*. (2023) presented a refined spectral element model for wave propagation in multiscale hybrid epoxy/carbon fiber/graphene platelet composite shells subjected to impulsive loadings. Hua *et al*. (2024) proposed a semi-analytical spectral element model combining the Fourier series and higher-order polynomials for wave propagation in composite laminated conical shells. Hua *et al*. (2022) investigated wave propagation in functionally graded (FG) viscoelastic polymer composite shells reinforced with spherical graphite particles (SGPs). The wave propagation characteristics in GPLs reinforced plates were scrutinized by Li *et al*. (2020) utilizing a semi-analytical approach. Furthermore, investigating the propagation of elastic waves in a square plate is investigated by Gao *et al*. (2020). The plate is reinforced by porous GPLs. The classical mechanical theory is employed and the material properties are described using the Halpin Tsai model. Additionally, Ebrahimi *et al*. (2019 and 2021) studied the wave propagation of porous GPLs reinforced composite shells using classical mechanics theory and Reddy's high-order shear deformation theory. Also, they studied the wave propagation behavior of a size-dependent graphene nanoplatelet-reinforced composite (GNPRC) nano-shell. Furthermore, rotating FG microbeams strengthened by graphene nanoplatelets (GPLs) are investigated by Zhao *et al*. (2021). The application of the classical mechanical theory is the main focus of the studies on wave propagation

*Corresponding author, Ph.D.,
E-mail: bendida65@gmail.com
**Co-corresponding author, Professor,
E-mail: tou_abdel@yahoo.com

ISSN: 2287-237X (Print), 2287-2388 (Online)

described earlier of structures (plates and shells). It is crucial to note, too, that there is a dearth of research on structures in this paradigm that are reinforced by GPNs or GPLs using non-local theory. Ebrahimi and Dabbagh (2018) addressed the wave propagation properties in nanoplates reinforced by graphene plates (GPL) in their paper. The unique singular size parameter inherent to nonlocal theory plays a pivotal role in elucidating nonlocal phenomena within material behavior, offering crucial insights into wave propagation, deformation, and fracture mechanics at miniature scales. However, it's noteworthy that while this hypothesis explains the stiffness softening effect, it does not account for the stiffness strengthening effect, rendering it unable to fully characterize the mechanical properties in some nanostructures. It's pertinent to differentiate nonlocal strain gradient (NSG) theory (Lim *et al.* 2015) from conventional classical theory (Hadji *et al*. 2018, Moradi and Mansouri 2012) and non-classical theories such as non-local theory (Eringen 1998, Ansari *et al*. 2016, Civalek and Demir 2016, Barretta and De Sciarra 2018, Malikan *et al*. 2018, Emam *et al*. 2018, Uzun and Civalek 2019, Taherifar *et al*. 2019, Barretta *et al*. 2019, Eltaher *et al*. 2020, Almitani *et al*. 2020) nonlocal couple stress theory (Attia and Mahmoud 2016, Attia 2017, Eltaher and Abdelrahman 2020, Vantadori *et al*. 2022, Ebrahimi *et al*. 2020), doublet mechanics (Eltaher and Mohamed 2020), and modified couple stress theory (Akgöz and Civalek 2017a, b). Supported by molecular dynamics and experiments, NSG theory (Lim *et al*. 2015, She *et al*. 2020, Apuzzo *et al*. 2018, Barretta and De Sciarra 2018, Lu *et al*. 2018, Faleh *et al*. 2018, Ghayesh and Farajpour 2018, Ghayesh *et al*. 2019, Gao *et al*. 2019, Pinnola *et al*. 2020, Malikan *et al*. 2020, She 2020) comprehensively characterizes both the stiffness strengthening and softening effects, significantly contributing to the development of nanomechanics theory.

In this research, the dynamics of elastic wave propagation within polymer composite nanoplates strengthened by graphene nanoplatelets, which are situated on variable elastic foundations are investigated. the nonlocal strain gradient theory is employed as the framework for our investigation. A four-variable displacement field is integrated and small-scale effects are handled. The dispersion relations and the non-classical wave equation are derived using the trial function and the Hamilton principle. The study's goals are to identify the effects of various parameters on the behavior of wave propagation. By considering the influence of small-scale effects and employing advanced mathematical frameworks like nonlocal strain gradient theory, the study endeavors to enhance our understanding of wave behavior in nano-materials. Also, the aim of this research is to unravel key axes that will help to control wave propagation in these structures and create new materials with specific mechanical properties for a variety of industrial applications. Overall, the novelty of this work lies in its unique combination of advanced theoretical models, innovative material reinforcement, and comprehensive parameter analysis, which together provide new insights into the wave propagation behavior of reinforced nanoplates on elastic foundations. These findings have the potential to significantly advance the design and application of nanocomposite materials in various engineering fields.

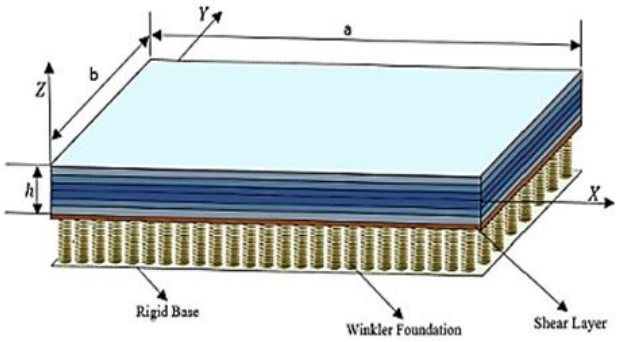

Fig. 1 GNP-reinforced FG nanoplate (Aditya *et al*. 2019)

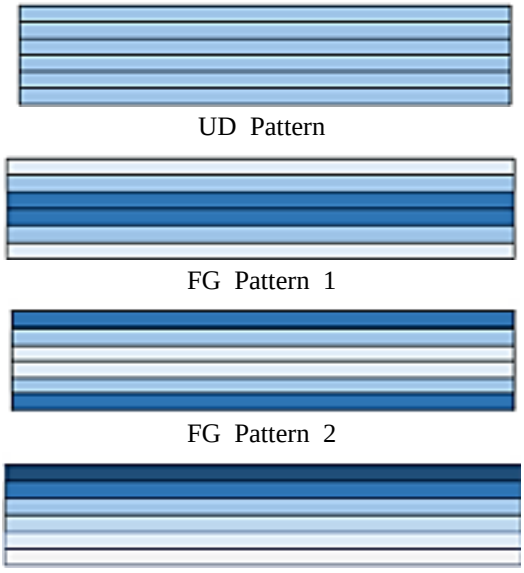

Fig. 2 Patterns of FG materials

2. Mathematical formulations

In this section, the basic formulation of the wave propagation problem for polymer nanoplates reinforced with GNPs is outlined. The NSGT with a four variable higher order shear deformation theory are used.

The functionally graded polymer composite nanoplate is constructed with N_L layers, each having a thickness of $h = h/N_L$ and has dimensions of a, b, and has represented in Fig. 1. Distributions (UD pattern, FG pattern 1, FG pattern 2, and FG pattern 3) that define GNPs as filler inside each layer is shown in Fig. 2. To be more precise, in a UD (Uniform Distribution) pattern, GNPs are evenly distributed. In contrast, in a FG (Functionally Graded) pattern 1 distribution, the highest weight fraction of GNPs is located at the center of the nanoplate. In a FG pattern 2, the middle level of the nanoplate is where the smallest weight fraction is reached while the top and bottom sides are where the greatest weight is reached. Furthermore, in FG Pattern 3, there is an increasing weight fraction of GNPs moving from the bottom to the top side of the nanoplate.

The material properties of the nanoplate are computed using the Halpin-Tsai model as described in reference (She 2020).

$$Ec=\frac{3Em}{8}\left[1-\frac{1+\frac{2l_{Gnp}}{h_{Gnp}}\left(\frac{\frac{E_{Gnp}}{Em}-1}{\frac{E_{Gnp}}{Em}+2\frac{l_{Gnp}}{h_{Gnp}}}\right)\left(\frac{g_{Gnp}}{g_{Gnp}+\left(\frac{\rho_{Gnp}}{\rho_m}\right)(1-g_{Gnp})}\right)}{\left(\frac{\frac{E_{Gnp}}{Em}-1}{\frac{E_{Gnp}}{Em}+2\frac{l_{Gnp}}{h_{Gnp}}}\right)\left(\frac{g_{Gnp}}{g_{Gnp}+\left(\frac{\rho_{Gnp}}{\rho_m}\right)(1-g_{Gnp})}\right)}\right] \quad (1)$$

$$\frac{5Em}{8}\left[\frac{1+\frac{2w_{Gnp}}{h_{Gnp}}\left(\frac{\frac{E_{Gnp}}{Em}-1}{\frac{E_{Gnp}}{Em}+2\frac{w_{Gnp}}{h_{Gnp}}}\right)\left(\frac{g_{Gnp}}{g_{Gnp}+\left(\frac{\rho_{Gnp}}{\rho_m}\right)(1-g_{Gnp})}\right)}{1-\left(\frac{\frac{E_{Gnp}}{Em}-1}{\frac{E_{Gnp}}{Em}+2\frac{L_{Gnp}}{h_{Gnp}}}\right)\left(\frac{g_{Gnp}}{g_{Gnp}+\left(\frac{\rho_{Gnp}}{\rho_m}\right)(1-g_{Gnp})}\right)}\right]$$

$$\rho_c=\rho_{Gnp}\left(\frac{g_{Gnp}}{g_{Gnp}+\left(\frac{\rho_{Gnp}}{\rho_m}\right)(1-g_{Gnp})}\right)+\rho_m\left(\frac{g_{Gnp}}{g_{Gnp}+\left(\frac{\rho_{Gnp}}{\rho_m}\right)(1-g_{Gnp})}\right) \quad (2)$$

$$V_c=V_{Gnp}\left(\frac{g_{Gnp}}{g_{Gnp}+\left(\frac{\rho_{Gnp}}{\rho_m}\right)(1-g_{Gnp})}\right)+V_m\left(\frac{g_{Gnp}}{g_{Gnp}+\left(\frac{\rho_{Gnp}}{\rho_m}\right)(1-g_{Gnp})}\right) \quad (3)$$

The Young's modulus of both the polymeric matrix and nanofillers is presented here by Em and $E_{Gnp}.\rho_m$ and ρ_{Gnp} are the mass density of the polymeric matrix and nanofillers, the polymeric matrix and nanofillers' Poisson's ratio is represented by V_m and V_{Gnp}. The average dimensions of length, width, and thickness of the GNPs are denoted by the specified parameters l_{Gnp}, w_{Gnp}, h_{Gnp} respectively. Additionally, the representation of the weight fraction of the GNP polymer nanocomposite for the k-layer is denoted by the specified symbol $g_{gnp}^{(k)}$. Here, we look at four different types of GNP distribution with:

$$g_{gnp}^{(k)}=\begin{cases} g_{Gnp}^{*} & \text{UD Pattern} \\ \frac{4g_{Gnp}^{*}\left(\frac{N_L+1}{2}-\left|k-\frac{N_L+1}{2}\right|\right)}{(2+N_L)} & \text{FG Pattern1} \\ \frac{4g_{Gnp}^{*}\left(\frac{1}{2}-\left|k-\frac{N_L+1}{2}\right|\right)}{(2+N_L)} & \text{FG Pattern2} \\ \frac{2kg_{Gnp}^{*}}{(N_L+1)} & \text{FG Pattern3} \end{cases} \quad (4)$$

g_{Gnp}^{*} being the GNPs' weight percentage.

2.1 Kinematics and constitutive equation

The displacement field of the higher order four variable plate theory is represented in the following manner (Thai *et al*. 2013):

$$u(x,y,z,t)=u_0(x,y,t)-z\frac{\partial w_b}{\partial x}-f(z)\frac{\partial w_s}{\partial x} \quad (5a)$$

$$v(x,y,z,t)=v_0(x,y,t)-z\frac{\partial w_b}{\partial y}-f(z)\frac{\partial w_s}{\partial y} \quad (5b)$$

$$w(x,y,z,t)=w_b(x,y,t)+w_s(x,y,t) \quad (5c)$$

The mid-plane displacements of the plate in the x and y directions are denoted as u_0 and v_0, respectively, while the bending and shear components of transverse displacement are represented by w_b and w_s, respectively. Furthermore, the shape function $f(z)$ is defined as follows:

$$f(z)=z-\frac{h}{\pi}sin\left(\frac{\pi z}{h}\right) \quad (6)$$

Using the displacement field described in Eq. (5), both normal and shear strains are calculated as follows:

$$\begin{Bmatrix}\varepsilon_x\\ \varepsilon_y\\ \gamma_{xy}\\ \gamma_{yz}\\ \gamma_{xz}\end{Bmatrix}=\begin{Bmatrix}\varepsilon_x^0+z\,k_x^b+f(z)\,k_x^s\\ \varepsilon_y^0+z\,k_y^b+f(z)\,k_y^s\\ \gamma_{xy}^0+z\,k_{xy}^b+f(z)\,k_{xy}^s\\ g(z)\gamma_{yz}^s\\ g(z)\gamma_{xz}^s\end{Bmatrix} \quad (7)$$

where,

$$\begin{Bmatrix}\varepsilon_x^0\\ \varepsilon_y^0\\ \gamma_{xy}^0\end{Bmatrix}=\begin{Bmatrix}\frac{\partial u_0}{\partial x}\\ \frac{\partial v_0}{\partial x}\\ \frac{\partial u_0}{\partial y}+\frac{\partial v_0}{\partial x}\end{Bmatrix},\quad \begin{Bmatrix}k_x^b\\ k_y^b\\ k_{xy}^b\end{Bmatrix}=\begin{Bmatrix}-\frac{\partial^2 w_b}{\partial x^2}\\ -\frac{\partial^2 w_b}{\partial y^2}\\ -2\frac{\partial^2 w_b}{\partial x\partial y}\end{Bmatrix},$$
$$\begin{Bmatrix}k_x^s\\ k_y^s\\ k_{xy}^s\end{Bmatrix}=\begin{Bmatrix}-\frac{\partial^2 w_s}{\partial x^2}\\ -\frac{\partial^2 w_s}{\partial y^2}\\ -2\frac{\partial^2 w_s}{\partial x\partial y}\end{Bmatrix},\quad \begin{Bmatrix}\gamma_{yz}^s\\ \gamma_{xz}^s\end{Bmatrix}=\begin{Bmatrix}\frac{\partial w_s}{\partial y}\\ \frac{\partial w_s}{\partial x}\end{Bmatrix}, \quad (8a)$$

and

$$g(z)=1-\frac{df(z)}{dz} \quad (8b)$$

According to the NSG theory, the constitutive equation is given as (She *et al*. 2020, Apuzzo *et al*. 2018, Barretta and De Sciarra 2018, Lu *et al*. 2018, Faleh *et al*. 2018, Ghayesh and Farajpour 2018, Malikan *et al*. 2020, She 2020):

$$(1-\mu^2\nabla^2)\begin{Bmatrix}\sigma_x\\ \sigma_y\\ \tau_{yz}\\ \tau_{xz}\\ \tau_{xy}\end{Bmatrix}=(1-l^2\nabla^2)\begin{bmatrix}Q_{11}^{(k)} & Q_{12}^{(k)} & 0 & 0 & 0\\ Q_{12}^{(k)} & Q_{22}^{(k)} & 0 & 0 & 0\\ 0 & 0 & Q_{44}^{(k)} & 0 & 0\\ 0 & 0 & 0 & Q_{55}^{(k)} & 0\\ 0 & 0 & 0 & 0 & Q_{66}^{(k)}\end{bmatrix}\begin{Bmatrix}\varepsilon_x\\ \varepsilon_y\\ \gamma_{yz}\\ \gamma_{xz}\\ \gamma_{xy}\end{Bmatrix} \quad (9)$$

Here

$$Q_{11}^{(k)}=Q_{22}^{(k)}=\frac{E_c^{(k)}}{1-\left(v_c^{(k)}\right)^2}$$
$$Q_{12}^{(k)}=Q_{21}^{(k)}=v_c^{(k)}Q_{11}^{(k)} \quad (10)$$
$$Q_{44}^{(k)}=Q_{55}^{(k)}=Q_{55}^{(k)}=\frac{E_c^{(k)}}{2\left(1+v_c^{(k)}\right)}$$

The nonlocal and strain gradient parameters μ and l are utilized to explain the stiffness-softening and stiffness-hardening mechanisms of nanostructures, respectively.

2.2 Variable elastic foundation

The nanoplates resting on a variable foundation is the subject of the current investigation. The spring-like action and the shear interaction are the two main foundation model utilized. Implementing the two-parameter reaction described on the nanoplate facilitates the formulation to account for these two phenomena, as depicted in Fig. 1. The foundation's reaction force density is described as follows:

$$f_e = K_w(x)\, w(x,y) - K_G \nabla^2 w(x,y) \tag{11}$$

where K_w is the Winkler parameter that depends only on x. It can be linear, parabolic, or sinusoidal, as described below (Sobhy 2015):

$$K_w(x) = \frac{J_1 h^3}{a^4}\begin{cases} 1+\xi\left(\frac{x}{a}\right) & \text{Linear,} \\ 1+\xi\left(\frac{x}{a}\right)^2 & \text{Parabolic,} \\ 1+\xi\, sin\left(\pi\frac{x}{a}\right) & \text{Sinusoidal,} \end{cases} \tag{12}$$

In this expression, J_1 remains constant while ξ varies. K_G denotes the stiffness of the shear layer foundation, and ∇^2 represents the Laplace operator in both x and y directions. It's worth noting that when ξ equals zero, the elastic foundation shifts to a Pasternak foundation, and if the stiffness of the shear layer foundation is ignored, the Pasternak foundation becomes equivalent to the Winkler foundation.

2.3 Governing equations

According to the Hamilton principle (Panda and Singh 2013, Singh and Panda 2014, Akbas 2015, Selmi 2020, Sahu *et al*. 2020, Vinyas 2020, Esen *et al*. 2023, Shanab *et al*. 2023, Abdelrahman *et al*. 2024)

$$\int_0^t (\delta U + \delta V - \delta K)\, dt = 0 \tag{13}$$

The expression for the virtual strain energy can be stated as follows:

$$\delta U = \int_A \begin{bmatrix} N_x \delta\, \varepsilon_x^0 + N_y \delta\, \varepsilon_y^0 + N_{xy} \delta\, \varepsilon_{xy}^0 + M_x^b \delta\, k_x^b \\ +M_y^b \delta\, k_y^b + M_{xy}^b \delta\, k_{xy}^b + M_x^s \delta\, k_x^s + M_y^s \delta\, k_y^s \\ +M_{xy}^s \delta\, k_{xy}^s + S_{yz}^s \gamma_{yz}^s + S_{xz}^s \gamma_{xz}^s \end{bmatrix} d\,A \tag{14}$$

A is the top surface,

The stress resultants: N, M and S can be expressed as follows:

$$\{N_x \quad N_y \quad N_{xy}\} = \int_{-h/2}^{h/2} (\sigma_x, \sigma_y, \tau_{xy})\, dz$$
$$\{M_x^b \quad M_y^b \quad M_{xy}^b\} = \int_{-h/2}^{h/2} (\sigma_x, \sigma_y, \tau_{xy})\, z dz \tag{15a}$$

$$\{M_x^s \quad M_y^s \quad M_{xy}^s\} = \int_{-h/2}^{h/2} (\sigma_x, \sigma_y, \tau_{xy}) f(z) dz \tag{15b}$$

$$(S_{xz}^s, S_{yz}^s) = \int_{-h/2}^{h/2} (\tau_{xz}, \tau_{yz})\, g(z) dz$$

After replacing Eq. (9) with Eq. (15) and integrating over the thickness of the plate, the stress resultants can be determined.

$$\begin{Bmatrix} \begin{Bmatrix} N_x \\ N_y \\ N_{xy} \end{Bmatrix} \\ \begin{Bmatrix} M_x^b \\ M_y^b \\ M_{xy}^b \end{Bmatrix} \\ \begin{Bmatrix} M_x^s \\ M_y^s \\ M_{xy}^s \end{Bmatrix} \end{Bmatrix} = \begin{bmatrix} \begin{bmatrix} A_{11} & A_{12} & 0 \\ A_{12} & A_{22} & 0 \\ 0 & 0 & A_{66} \end{bmatrix} & \begin{bmatrix} B_{11} & B_{12} & 0 \\ B_{12} & B_{22} & 0 \\ 0 & 0 & B_{66} \end{bmatrix} & \begin{bmatrix} B_{11}^s & B_{12}^s & 0 \\ B_{12}^s & B_{22}^s & 0 \\ 0 & 0 & B_{66}^s \end{bmatrix} \\ \begin{bmatrix} B_{11} & B_{12} & 0 \\ B_{12} & B_{22} & 0 \\ 0 & 0 & B_{66} \end{bmatrix} & \begin{bmatrix} D_{11} & D_{12} & 0 \\ D_{12} & D_{22} & 0 \\ 0 & 0 & D_{66} \end{bmatrix} & \begin{bmatrix} D_{11}^s & D_{12}^s & 0 \\ D_{12}^s & D_{22}^s & 0 \\ 0 & 0 & D_{66}^s \end{bmatrix} \\ \begin{bmatrix} B_{11}^s & B_{12}^s & 0 \\ B_{12}^s & B_{22}^s & 0 \\ 0 & 0 & B_{66}^s \end{bmatrix} & \begin{bmatrix} D_{11}^s & D_{12}^s & 0 \\ D_{12}^s & D_{22}^s & 0 \\ 0 & 0 & D_{66}^s \end{bmatrix} & \begin{bmatrix} H_{11}^s & H_{12}^s & 0 \\ H_{12}^s & H_{22}^s & 0 \\ 0 & 0 & H_{66}^s \end{bmatrix} \end{bmatrix} \begin{Bmatrix} \begin{Bmatrix} \varepsilon_x^0 \\ \varepsilon_y^0 \\ \gamma_{xy}^0 \end{Bmatrix} \\ \begin{Bmatrix} k_x^b \\ k_y^b \\ k_{xy}^b \end{Bmatrix} \\ \begin{Bmatrix} k_x^s \\ k_y^s \\ k_{xy}^s \end{Bmatrix} \end{Bmatrix} \tag{15c}$$

$$\begin{Bmatrix} S_{yz}^s \\ S_{xz}^s \end{Bmatrix} = \begin{bmatrix} A_{44}^s & 0 \\ 0 & A_{55}^s \end{bmatrix} \begin{Bmatrix} \gamma_{yz}^0 \\ \gamma_{xz}^0 \end{Bmatrix} \tag{15d}$$

and stiffness components are given as:

$$(A_{ij}, B_{ij}, B_{ij}^s, D_{ij}, D_{ij}^s, H_{ij}^s) = \sum_{k=1}^{N_l} \int_{z(k)}^{z(k+z)} Q^k{}_{ij} (1, z, f(z), z^2, zf(z), f(z)^2) dz\,, \quad (i,j = 1,2,6), \tag{16a}$$

$$A_{44}^s = \sum_{k=1}^{N_l} \int_{z(k)}^{z(k+z)} Q^k{}_{44} \left[g(z)\right]^2 dz\,,$$
$$A_{55}^s = \sum_{k=1}^{N_l} \int_{z(k)}^{z(k+z)} Q^k{}_{55} [g(z)]^2 dz, \tag{16b}$$

The foundation response alone is what causes the external work to be applied to the nanoplate. Consequently, the initial iteration of the external work is provided by (Rachedi *et al*. 2020, Merzoug *et al*. 2020, Timesli 2020)

$$\delta V = f_e \delta w = \int_A \begin{pmatrix} K_w(x) w(x,y,t) \\ -K_G \nabla^2 w(x,y,t) \end{pmatrix} \delta w d\Omega \tag{17}$$

For the wave propagation problem, the initial variation of the kinetic energy is provided by:

$$\delta K = \int_A \int_{-h/2}^{h/2} \frac{1}{2} \int_V \rho(z)[\dot{u}\delta\dot{u} + \dot{v}\delta\dot{v} + \dot{w}\delta\dot{w}] dz dA \tag{18}$$

By substituting Eq. (7) into Eq. (9) and applying Eqs. (13) and (5), equations of motion for the nanoplate can be obtained as follows:

$$(1 - l^2\nabla^2) \begin{pmatrix} (A_{11}) d_{11} u_0 + (A_{66}) d_{22} u_0 \\ +(A_{12} + A_{66}) d_{12} v_0 \\ -(B_{11}) d_{111} w_b - (B_{11}^s) d_{111} w_s \\ -(B_{12} + 2B_{66}) d_{122} w_b \\ -(B_{12}^s + 2B_{66}^s) d_{122} w_s \end{pmatrix} = (1 - \mu^2\nabla^2)(I_0 \ddot{u}_0 - I_1 d_1 \ddot{w}_b - J_1 d_1 \ddot{w}_s), \tag{19a}$$

$$(1-l^2\nabla^2)\begin{pmatrix}(A_{22})d_{22}v_0+(A_{66})d_{11}v_0\\+(A_{12}+A_{66})d_{12}u_0\\-(B_{22})d_{222}w_b-(B^s_{22})d_{222}w_s\\-(B_{12}+2B_{66})d_{112}w_b\\-(B^s_{12}+2B^s_{66})d_{112}w_s\end{pmatrix} = (1-\mu^2\nabla^2)(I_0\ddot{v}_0-I_1d_2\ddot{w}_b-J_1d_2\ddot{w}_s), \tag{19b}$$

$$(1-l^2\nabla^2)\begin{pmatrix}(B_{11})d_{111}u_0+(B_{12}+2B_{66})d_{122}u_0\\+(B_{12}+2B_{66})d_{112}v_0+(B_{22})d_{222}v_0-\\(D_{11})d_{1111}w_b-(D^s_{11})d_{1111}w_s\\-2(2D_{66}+D_{12})d_{1122}w_b\\-2(D^s_{12}+2D^s_{66})d_{1122}w_s\\-(D_{22})d_{2222}w_b-(D^s_{22})d_{2222}w_s\end{pmatrix} + (1-\mu^2\nabla^2)(K_ww-K_G\nabla^2w) = (1-\mu^2\nabla^2)\begin{pmatrix}I_0(\ddot{w}_b+\ddot{w}_s)+I_1(d_1\ddot{u}_0+d_2\ddot{v}_0)\\-I_2(d_{11}\ddot{w}_b+d_{22}\ddot{w}_b)\\-J_2(d_{11}\ddot{w}_s+d_{22}\ddot{w}_s)\end{pmatrix} \tag{19c}$$

$$(1-l^2\nabla^2)\begin{pmatrix}(B^s_{11}+B^s_{11})d_{111}u_0\\+(B^s_{12}+2B^s_{66})d_{122}u_0\\+(B^s_{12}+2B^s_{66})d_{112}v_0+(B^s_{22})d_{222}v_0\\-(D^s_{11})d_{1111}w_b-(H^s_{11})d_{1111}w_s\\-2(2D^s_{66}+D^s_{12})d_{1122}w_b\\-(D^s_{22})d_{2222}w_b-\\2(H^s_{12}+2H^s_{66})d_{1122}w_s-(H^s_{22})d_{2222}w_s\\+A^s_{44}d_{22}w_s+A^s_{55}d_{11}w_s+\end{pmatrix} + (1-\mu^2\nabla^2)(K_ww-K_G\nabla^2w) = (1-\mu^2\nabla^2)\begin{pmatrix}I_0(\ddot{w}_b+\ddot{w}_s)+J_1(d_1\ddot{u}_0+d_2\ddot{v}_0)-\\J_2(d_{11}\ddot{w}_b+d_{22}\ddot{w}_b)\\-K_2(d_{11}\ddot{w}_s+d_{22}\ddot{w}_s)\end{pmatrix} \tag{19d}$$

The operators d_{ij}, d_{ijl} and d_{ijlm} are defined as:

$$d_{ij}=\frac{\partial^2}{\partial x_i\partial x_j},\quad d_{ijl}=\frac{\partial^3}{\partial x_i\partial x_j\partial x_l},\ d_{ijlm}=\frac{\partial^4}{\partial x_i\partial x_j\partial x_l\partial x_m},\quad d_i=\frac{\partial}{\partial x_i},\ (i,j,l,m=1,2). \tag{20}$$

The inertias are represented by:

$$(I_0,I_1,J_1,I_2,J_2,K_2)=\sum_{k=1}^{N_l}\int_{z(k)}^{z(k+z)}(1,z,f,z^2,zf,f^2)dz\rho_c^{(k)} \tag{21}$$

2.4 Dispersion relation

To resolve the issue of wave propagation, we assume:

$$\begin{Bmatrix}u_0\\v_0\\w_b\\w_s\end{Bmatrix}=\begin{Bmatrix}Ue^{[i(\kappa_1x+\kappa_2y-\omega t)]}\\Ve^{[i(\kappa_1x+\kappa_2y-\omega t)]}\\W_be^{[i(\kappa_1x+\kappa_2y-\omega t)]}\\W_se^{[i(\kappa_1x+\kappa_2y-\omega t)]}\end{Bmatrix} \tag{22}$$

U, V, W_b and W_s represent constant amplitude coefficients of the propagating wave. κ_1 and κ_2 denote the wavenumbers in the x and y directions, respectively, while ωstands for the wave frequency, with i being the imaginary unit. This solution is then applied to the equations of motion. The resulting equations involve five unknowns: U, V, W_b and W_s and ω . Each term may appear squared or within the exponential function. The four equations of motion are then simplified into a matrix form.

$$\left(\beta\begin{bmatrix}a_{11}&a_{12}&a_{13}&a_{14}\\a_{21}&a_{22}&a_{23}&a_{24}\\a_{31}&a_{32}&a_{33}&a_{34}\\a_{41}&a_{42}&a_{43}&a_{44}\end{bmatrix}-\alpha\omega^2\begin{bmatrix}m_{11}&0&m_{13}&m_{14}\\0&m_{22}&m_{23}&m_{24}\\m_{31}&m_{32}&m_{33}&m_{34}\\m_{41}&m_{42}&m_{43}&m_{44}\end{bmatrix}\right)\begin{Bmatrix}U\\V\\W_b\\W_s\end{Bmatrix}=\begin{Bmatrix}0\\0\\0\\0\end{Bmatrix} \tag{23}$$

in which:

$$\begin{aligned}
a_{11}&=-\kappa_1^2A_{11}-\kappa_2^2A_{66}\\
a_{12}&=-\kappa_1\kappa_2\left(A_{12}+A_{66}\right)\\
a_{13}&=i\kappa_1\left(\kappa_1^2B_{11}+\kappa_1\kappa_2^2\left(B_{12}+2B_{66}\right)\right)\\
a_{31}&=-i\kappa_1\left(\kappa_1^2B_{11}+\kappa_1\kappa_2^2\left(B_{12}+2B_{66}\right)\right)\\
a_{14}&=i\kappa_1\left[B^s_{11}\kappa_1^2+\left(B^s_{12}+2B^s_{66}\right)\kappa_2^2\right]\\
a_{41}&=i\kappa_1\left[B^s_{11}\kappa_1^2+\left(B^s_{12}+2B^s_{66}+\right)\kappa_2^2\right]\\
a_{22}&=-\kappa_1^2A_{66}-\kappa_2^2A_{22}\\
a_{23}&=i\kappa_2\left[\kappa_2^2B_{22}+\left(B_{12}+2B_{66}\right)\kappa_1^2\right]\\
a_{32}&=-i\kappa_2\left[\kappa_2^2B_{22}+\left(B_{12}+2B_{66}\right)\kappa_1^2\right]\\
a_{24}&=i\kappa_2\left[\kappa_2^2B^s_{22}+\left(B^s_{12}+2B^s_{66}\right)\kappa_1^2\right]\\
a_{33}&=-\left[D_{11}\kappa_1^4+2\left(D_{12}+2D_{66}\right)\kappa_1^2\kappa_2^2+D_{22}\kappa_2^4+\frac{\alpha}{\beta}\left(\overline{K}_W+K_G(\kappa_1^2+\kappa_2^2)\right)\right]\\
a_{34}&=-\left[D^s_{11}\kappa_1^4+2\left(D^s_{12}+2D^s_{66}\right)\kappa_1^2\kappa_2^2+D^s_{22}\kappa_2^4+\frac{\alpha}{\beta}\left(\overline{K}_W+K_G(\kappa_1^2+\kappa_2^2)\right)\right]\\
a_{44}&=-\Big[H^s_{11}\kappa_1^4+\left(2\left(H^s_{12}+2H^s_{66}\right)\right)\kappa_1^2\kappa_2^2+H^s_{22}\kappa_2^4\\
&\quad+A^s_{55}\kappa_1^2+A^s_{44}\kappa_2^2+\frac{\alpha}{\beta}\left(\overline{K}_W+K_G(\kappa_1^2+\kappa_2^2)\right)\Big]
\end{aligned} \tag{24}$$

$$\begin{aligned}
m_{11}&=I_1\\
m_{12}&=0\\
m_{13}&=-iI_2\kappa_1\\
m_{31}&=iI_2\kappa_1\\
m_{14}&=-iI_4\kappa_1\\
m_{41}&=iI_4\kappa_1\\
m_{22}&=I_1\\
m_{23}&=-iI_2\kappa_2\\
m_{32}&=-iI_2\kappa_2\\
m_{24}&=-iI_4\kappa_2\\
m_{42}&=iI_4\kappa_2\\
m_{33}&=I_1+I_3(\kappa_2^2+\kappa_1^2)\\
m_{34}&=I_1+I_5(\kappa_2^2+\kappa_1^2)\\
m_{44}&=I_1+I_6(\kappa_2^2+\kappa_1^2)\\
\alpha&=1+\mu(\kappa_2^2+\kappa_1^2)\\
\alpha&=1+l(\kappa_2^2+\kappa_1^2)\\
\overline{K}_W&=\int_0^a K_W dx\,/a
\end{aligned}$$

Using the following formulas, one may determine the phase velocity.

$$C_p=\frac{\omega}{k} \tag{25}$$

With $k_1=k_2=k$

3. Numerical results

Consider the polymer nanoplate shown in Fig. 1. Next, a thorough and methodical examination is conducted to

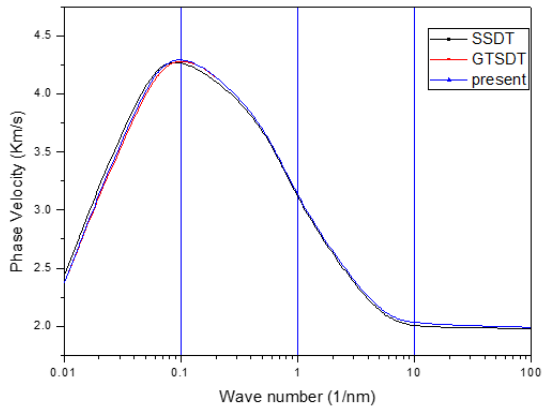

Fig. 3 Comparison of phase velocity in a rectangular nanoplate, (E=70GPa, ρ=2702 kg/m^3, ν=0.3, h=100 nm, μ=1 nm and l=0.2 nm)

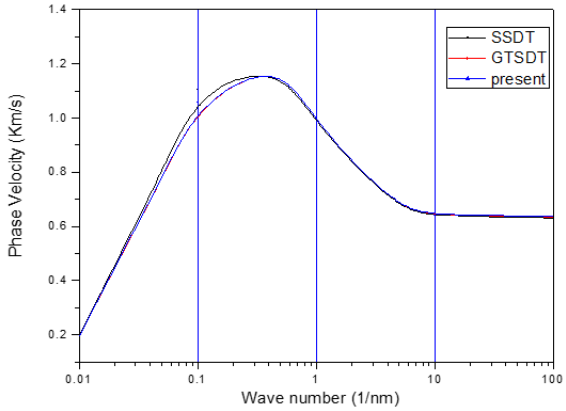

Fig. 4 Comparison of phase velocity for UD Pattern, ($g^*_{GNP} = 0.01$)

determine the effectiveness of nanoplates reinforced by GNPs in waves propagation. An epoxy matrix is considered with the following:

E= 3GPa, V_m= 0.34, et ρ_m = 1200 kg/m^3; E_{Gnp} = 1.01TPa, V_{Gnp} = 0.186, ρ_{Gnp} = 1060 kg/m^3; h = 20 nm.

Here, in Figs. 3 and 4 verification studies are conducted, and the results of the current wave propagation are compared to those of Karami *et al*. (2019) using the general third-order shear deformation theory (GTSDT) and She (2020) using the second shear deformation theory (SSDT). The outcomes exhibit a high level of consistency.

Various elasticity theories are utilized to explore the correlations among wave number and phase velocity in wave dispersion. The small parameter values in Fig. 5 are: $(\mu, l) = (0,0), (\mu, l) = (1nm, 0)$, $(\mu, l) = (1nm, 0)$ and $(\mu, l) = (1nm, 0.2nm)$ for the classical elasticity theory (CET), the nonlocal elasticity theory (NET), the strain gradient theory (SGT), and the nonlocal strain gradient theory (NSGT), respectively. The relationships between phase velocity and wave number for nanoplates seem to exhibit similarity across different patterns, including a UD pattern, FG pattern 1, FG pattern 2, and FG pattern 3. As predicted, the nonlocal parameter μ indicates a softening effect on stiffness, while the strain gradient parameter l shows a strengthening effect. The phase velocities from

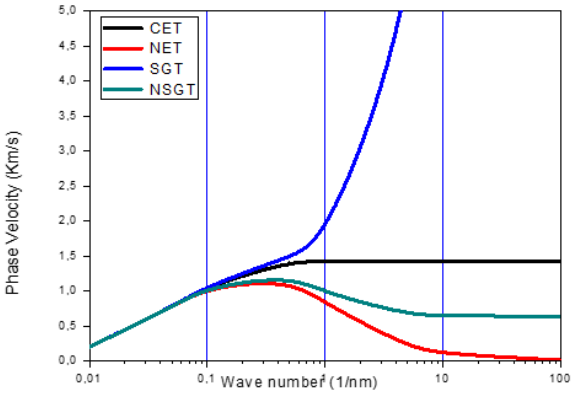

(a) UD Pattern

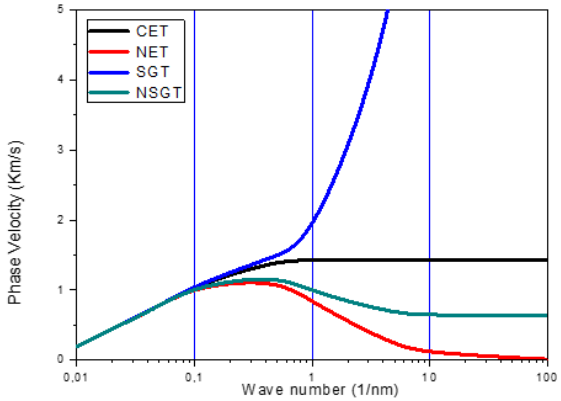

(b) FG Pattern

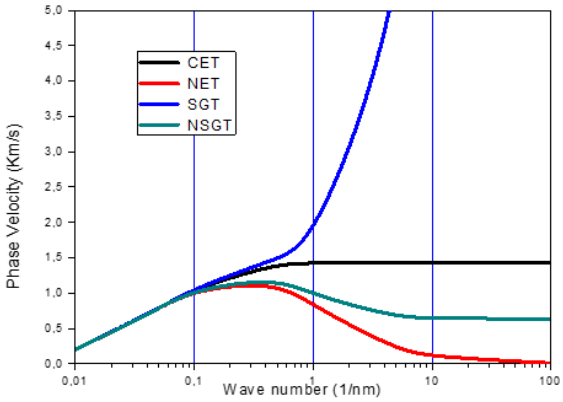

(c) FG Pattern 2

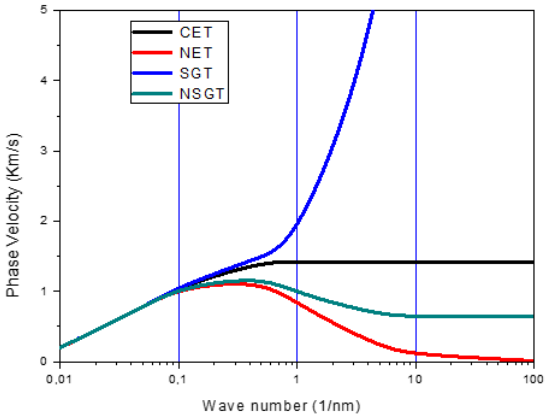

(d) FG Pattern 3

Fig. 5 Phase velocity dispersion relation for various theories at $g^*_{GNP} = 0.01$

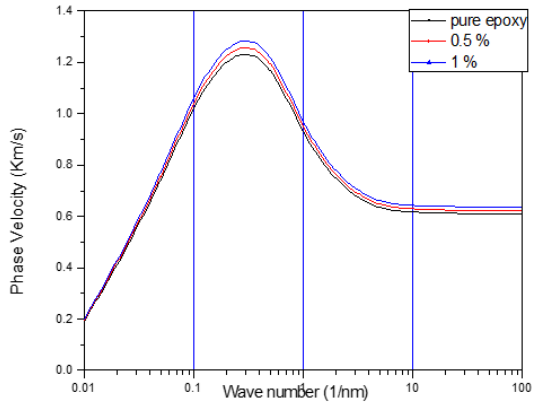

(a) UD Pattern

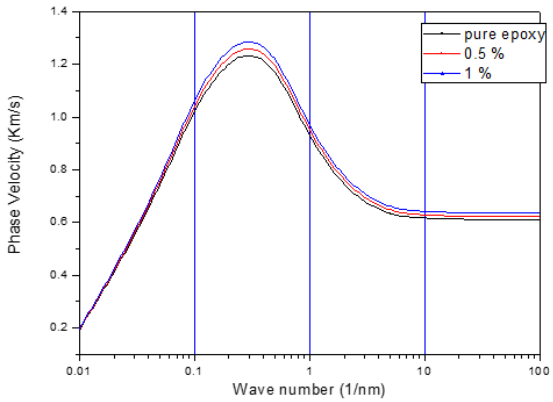

(b) FG Pattern

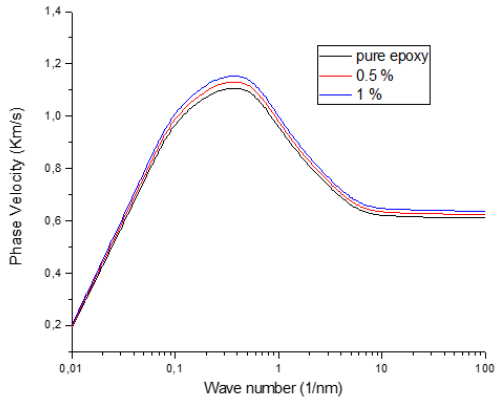

(c) FG Pattern 2

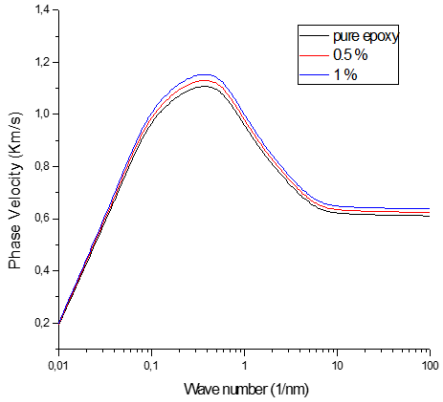

(d) FG Pattern 3

Fig. 6 Phase velocity dispersion relation for different weight fractions g^*_{GNP} (μ=1 nm and l=0.2 nm)

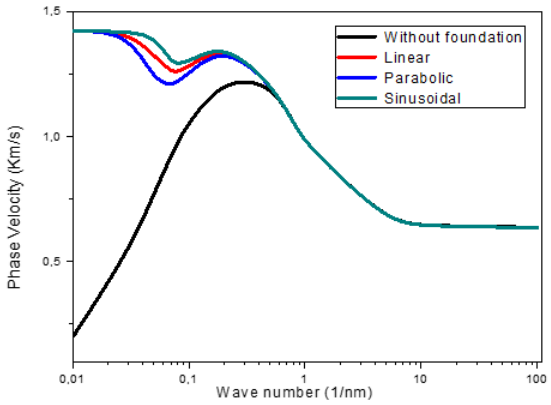

(a) UD Pattern

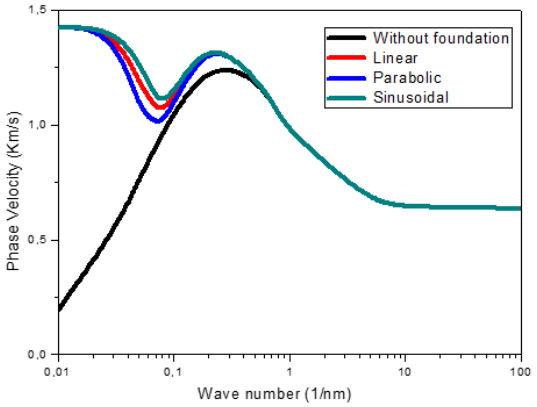

(b) FG Pattern

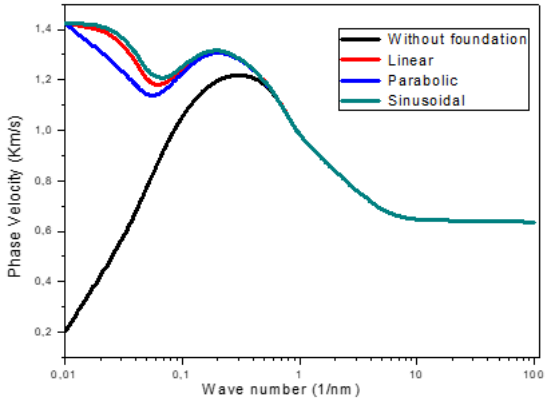

(c) FG Pattern 2

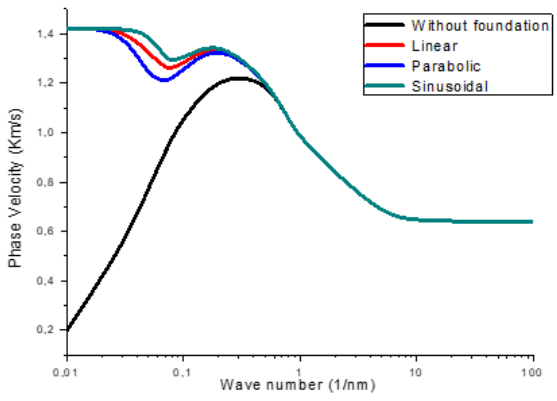

(d) FG Pattern 3

Fig. 7 Phase velocity dispersion relation for different types of Winkler parameter ($g^*_{GNP} = 0.01\mu$=1 nm and l=0.2 nm)

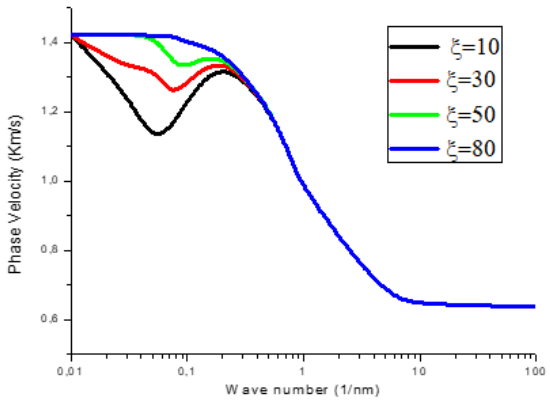

(a) UD Pattern

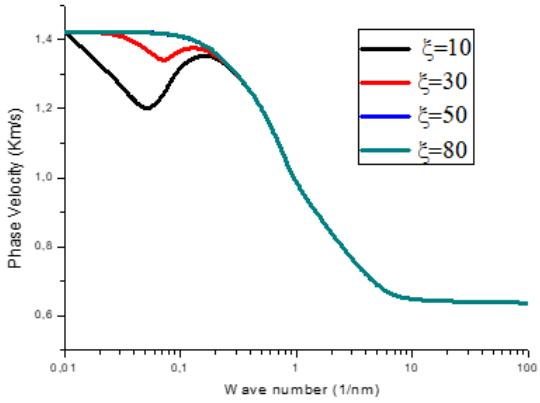

(b) FG Pattern

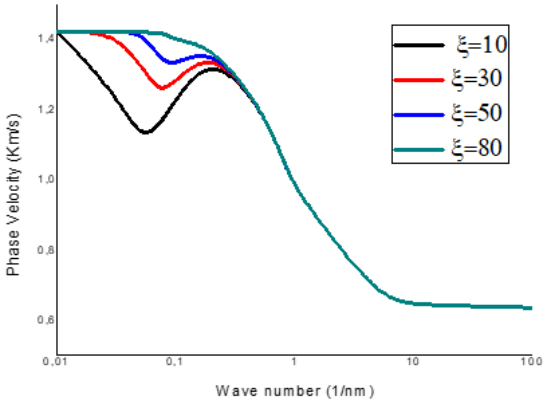

(c) FG Pattern 2

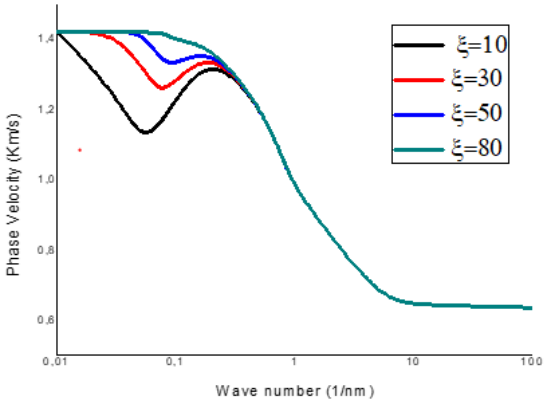

(d) FG Pattern 3

Fig. 8 Dispersion relation of the phase velocity for various for parabolic foundation (g^*_{GNP} = 0.01μ=1 nm and l=0.2 nm)

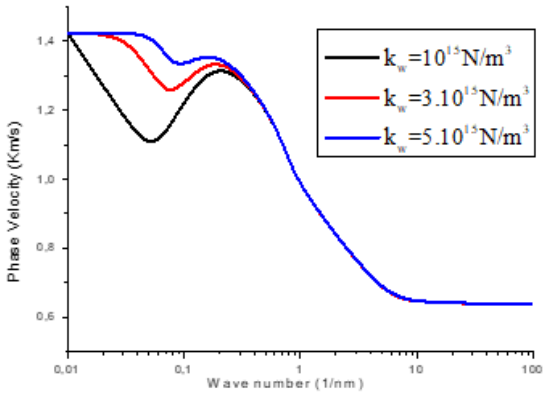

(a) UD Pattern

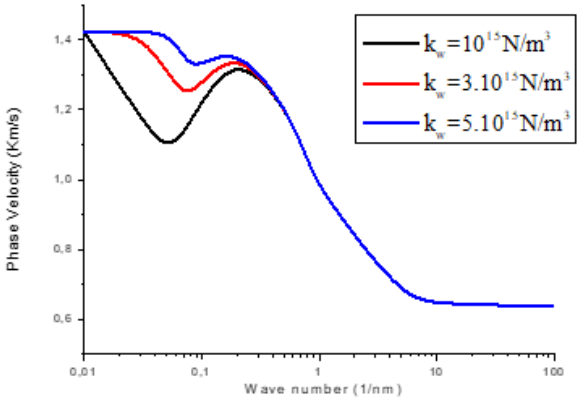

(b) FG Pattern

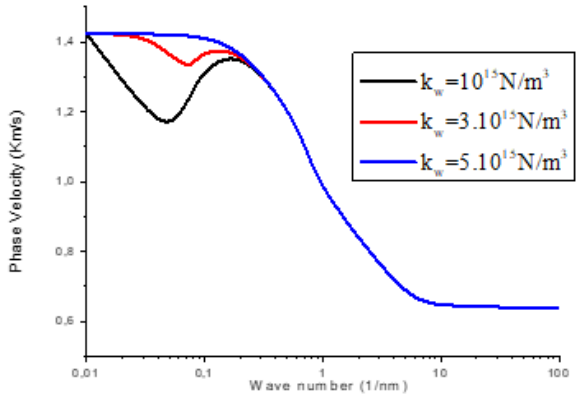

(c) FG Pattern 2

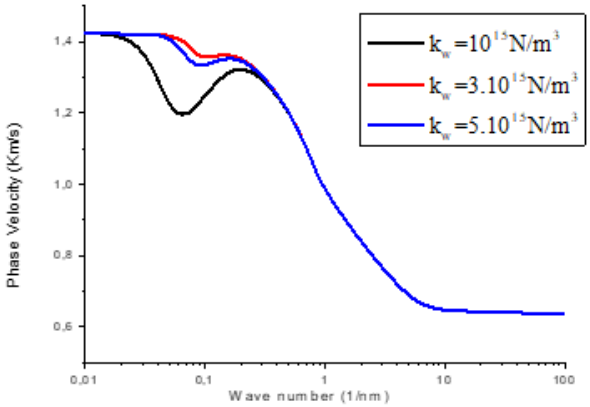

(d) FG Pattern 3

Fig. 9 Dispersion relation of the phase velocity for various for parabolic foundation (g^*_{GNP} = 0.01μ=1 nm and l=0.2 nm, ζ = 50, K_G = 4N/m)

Table 1 Naturel frequencies (GHZ) of FG pattern 1 for different wavenumbers κ $(k_w = 5.10^{15})$

(l,nu)	K_G (N/m)	ζ	$g^*_{GNP} = 0$			$g^*_{GNP} = 0.5\frac{0}{0}$			$g^*_{GNP} = 1\frac{0}{0}$		
			κ			κ			κ		
			0.05	0.07	0.1	0.05	0.07	0.1	0.05	0.07	0.1
(0,1)	0	0	39.580	63.533	116.54	40.163	64.658	104.59	40.739	65.765	106.61
		30	59.197	77.162	124.45	59.578	78.069	113.37	59.959	78.969	115.22
		50	68.125	85.000	129.44	69.514	85.814	118.85	69.837	86.622	120.59
		80	68.125	95.148	135.24	69.566	96.209	126.59	70.998	96.917	128.22
	4	0	48.409	74.437	116.54	48.881	75.381	118.32	49.351	76.317	120.07
		30	65.384	86.303	124.45	65.727	87.102	126.10	66.069	87.896	127.13
		50	68.125	93.338	129.44	69.566	94.067	131.01	70.998	94.795	132.56
		80	68.125	95.148	135.24	69.566	97.160	138.02	70.998	99.161	139.48
(0.2,0)	0	0	39.684	63.889	103.74	40.269	65.021	105.82	40.847	88.174	107.87
		30	59.267	77.455	112.61	59.650	78.370	114.51	60.033	76.636	116.38
		50	68.329	58.268	118.14	69.576	86.088	119.94	69.901	95.053	121.71
		80	68.329	95.706	125.95	69.774	96.456	127.62	71.211	99.743	129.27
	4	0	48.494	74.741	117.60	48.968	75.693	119.41	49.439	76.636	121.18
		30	65.448	86.566	125.45	65.792	87.373	127.12	66.137	88.174	128.78
		50	68.329	93.583	130.39	69.774	94.319	131.99	71.211	95.054	133.58
		80	68.329	95.706	136.86	69.774	97.731	138.96	71.211	99.743	140.44
(0.2,1)	0	0	39.597	63.593	102.74	40.181	64.719	104.79	40.757	65.827	106.82
		30	59.209	77.211	111.69	59.590	78.119	113.56	59.971	79.021	115.41
		50	68.159	85.045	117.26	69.524	85.859	119.03	69.848	86.669	120.78
		80	68.159	95.241	125.12	69.601	96.250	126.77	71.033	96.959	128.39
	4	0	48.423	74.487	116.72	48.895	75.434	118.49	49.365	76.371	120.26
		30	65.394	86.347	124.62	65.738	87.147	126.27	66.081	87.942	127.90
		50	68.159	93.379	129.59	69.601	94.109	131.17	71.034	94.838	132.73
		80	68.159	95.241	135.51	69.601	97.256	138.17	71.034	99.258	139.64

different continuum theories remain largely consistent for low wave numbers. An interesting finding is that when the wave number is below 0.1 1/nm, the phase velocities predicted by different elasticity models are essentially the same. This indicates that when$\kappa \succ 0.1$, various continuum theories result in various trends. Clearly, the size effects only function at sufficiently high wavenumbers. Moreover, when the conventional strain gradient theory is applied without considering nonlocal effects, the numerical results reveal a scenario where the phase velocity of the system becomes unbounded beyond a certain threshold of wave number. Additionally, it is observed that an increase in wave number beyond the peak value leads to a reduction in the phase velocity of the functionally graded nanoplate, particularly when the strain gradient parameter is smaller than the nonlocal parameters.

Diagrams of wave propagation for nanoplates with various weight fractions of g^*_{GNP} (=0, 0.5%, and 1%) and different patterns are shown in Fig. 6. As can be observed, as g^*_{GNP} increases, the phase velocity tends to rise as well.

Fig. 7 illustrates how different foundation models affect the relationship between phase velocity and wave number. Specifically, it shows nanoplates without any foundation support. $(K_W = K_G = 0)$ and elastic foundations $(K_G = 4N/m; K_W = 5 \times 10^{15} N/m^3; \zeta = 20)$. Three types of Winkler modulus are considered with linear, parabolic, and sinusoidal. The plot shown in Fig. 7 corresponds to a UD pattern, FG pattern 1, FG pattern 2, and FG pattern 3, with a total number of layers N_L = 10 and a nonlocal paramete$(\mu = 1nm)$, strain gradient parameter$(l = 0.2nm)$ and a weight fraction $(g_{GNP} = 1\%)$, illustrates the significant sensitivity of the reaction for changing Winkler modulus connected to the elastic foundation. The effect of changing Winkler modulus is more seen for FG pattern 1. In addition, when the wave number $\kappa\langle 0.1\ 1/nm$, the plate resting on a sinusoidal foundation exhibits the highest phase velocity.

Fig. 8 represents the variation of phase velocity in nanoplate resting on parabolic elastic foundation under the nonlocal and strain gradient effects is plotted in Fig. 8 for ζ = 10, 30, 50, 80. Generally, the phase velocities are almost identical for different parameter ζ after the certain value of wave number. Due to presented model, the fluctuations in

phase velocity prior to reaching a particular wave number are contingent upon the values of ζ. It is concluded that, the phase velocities become more affected by these parameter at lower wave numbers. Also the effect of the parameter ζ on the phase velocity disappear with greater values of ζ especially for the case of FG pattern 2.

Phase velocity of nanoplates resting on elastic foundation versus wave numbers for different values of K_W is plotted in Fig. 9 One can observe that increasing in the stiffness of elastic foundation parameters enhances the rigidity of nanoplates. On the other hand, when the wave number $\kappa\langle 0.1\ 1/nm$, As K_W increases, the curve becomes progressively flatter. Beyond a value of 5×10^15 for K_W, the curves become indistinguishable. In addition, it is seen that the influence of the Winkler parameter on the Phase velocity is more prominent in the case of UD pattern and FG pattern1. The effect of the Winkler parameter on phase velocity is more pronounced at low wave numbers because, at low wave numbers, the wavelength is longer, and the interaction between the plate and the foundation becomes more influential. The Winkler parameter, which models the stiffness of the foundation, affects the speed at which waves propagate through the material, resulting in a more noticeable impact on phase velocity. As the wave number increases, the wavelength decreases, and the effect of the foundation becomes less dominant compared to the material properties of the plate, thus reducing the influence of the Winkler parameter on phase velocity.

To serve as a benchmark, Table 1 presents the circular frequencies for the functionally graded polymer composite nanoplates resting on a two-parameter viscoelastic foundation with different parameter ζ, non local parameter μ, strain gradient parameter l, GNPs' weight percentage g^*_{GNP} and wave numbers. In this table, it can be noticed that the frequency increase with the increase of g^*_{GNP}. Also when the shear modulus K_G of the elastic foundation is not neglected the phase velocity decrease. The effect of non local parameterμ, strain gradient parameter$l$ is not seen for low wave numbers($\kappa = 0.05; 0.07; 0.1$). The effect of the parameter ζ is seen for low wave numbers.

4. Conclusions

In this work, the wave propagations of nanoplates reinforced with graphene nanoplatelets (GNPs) and featuring a functionally graded polymer composite structure are studied. The four variable shear deformation theory was used to develop the nonlocal strain gradient model for the nanoplates. The analyses of wave propagation are resolved using the trial function. It has been verified by comparing the results of this research with earlier discoveries. The dispersion relations between the wave propagation components are examined in this work. Numerical research reveals that the strain gradient parameter has the opposite influence on the wave's propagation velocity, including phase velocity, as the nonlocal parameters do. Furthermore, the various Winkler-foundation factors can all be used to increase the phase velocity of the nanoplates. The wave propagation velocity increases as weight fraction g_{GNP} increases. Examining the propagation characteristics in composite nanoplates made of functionally classified polymers reinforced with GNPs and supported by a variable elastic foundation is suggested. The studied material type can be extended and used in the others structures type with various external loading as (Daouadji and Hadji 2015, Eltaher *et al*. 2016, Ahmed *et al*. 2019, Avcar 2019, Eltaher *et al*. 2019, Mehar *et al*.2019, Mehar and Panda 2019, Al-Basyouni *et al*. 2019, Madenci 2019, Hadji 2020, Bharath *et al*. 2020, Abed and Majeed 2020, Madenci and Özütok 2020, Yahea and Majeed 2021, Hou *et al*. 2022, Behdinan and Moradi-Dastjerdi 2022, Turini and Calenzani 2022, Bochkareva and Lekomtsev 2022, Man 2022, Huang and Wu 2022, Yaylaci *et al*. 2023, Kim *et al*. 2023, Khatri and Markad 2023, Emdadi *et al*. 2023, Ding *et al*. 2023, Kamarian and Song 2023, Wu 2023, Tayebi *et al*. 2023, Sahoo *et al*. 2023, Mohamed *et al*. 2023, Turan 2023, Xu and Ming 2023, Janghorban and Tounsi 2024, Madenci *et al*. 2024, Tounsi *et al*. 2024, Xia *et al*. 2024).

Acknowledgments

This research work was funded by Institutional Fund Projects under grant no. (IFPIP_ 1569-135-1443). Therefore, the authors gratefully acknowledge technical and financial support from the Ministry of Education and King Abdulaziz University, Jeddah, Saudi Arabia.

References

Abdelrahman, A.A., Esen, I., Tharwan, M.Y., Assie, A. and Eltaher, M.A. (2024), "On vibrations of functionally graded carbon nanotube (FGCNT) nanoplates under moving load", *Adv. Nano Res.*, **16**(4), 395-412. https://doi.org/10.12989/anr.2024.16.4.395.

Abed Z.A.K. and Majeed, W.I. (2020), "Effect of boundary conditions on harmonic response of laminated plates", *Compos. Mater. Eng.*, **2**(2), 125-140. https://doi.org/10.12989/cme.2020.2.2.125.

Aditya, N.D., Ben, Z.T., Polit, O., Pradyumna B. and Ganapathi, M. (2019), "Large amplitude free flexural vibrations of functionally graded graphene platelets reinforced porous composite curved beams using finite element based on trigonometric shear deformation theory", *Int. J. Nonlinear. Mech.*, **116**, 302-317. https://doi.org/10.1016/j.ijnonlinmec.2019.07.010.

Ahmed, R.A., Fenjan, R.M., Faleh, N.M. (2019), "Analyzing post-buckling behavior of continuously graded FG nanobeams with geometrical imperfections", *Geomech. Eng.*, **17**(2), 175-180. https://doi.org/10.12989/gae.2019.17.2.175.

Akbas, S.D. (2015), "Wave propagation of a functionally graded beam in thermal environments", *Steel Compos. Struct.*, **19**(6), 1421-1447. https://doi.org/10.12989/SCS.2015.19.6.1421.

Akgöz, B. and Civalek, O. (2017), "A size-dependent beam model for stability of axially loaded carbon nanotubes surrounded by Pasternak elastic foundation", *Compos. Struct.*, **176**, 1028-1038. https://doi.org/10.1016/j.compstruct.2017.06.03

Akgöz, B. and Civalek, O. (2017b), "Effects of thermal and shear deformation on vibration response of functionally graded thick composite microbeams", *Compos. Part B: Eng.*, **129**, 77-87. https://doi.org/10.1016/j.compositesb.2017.07.024

Al-Basyouni, K.S., Ghandourah, E., Mostafa, H.M. and Algarni,

A. (2020), "Effect of the rotation on the thermal stress wave propagation in non-homogeneous viscoelastic body", *Geomech. Eng.*, **21**(1), 1-9. https://doi.org/10.12989/GAE.2020.21.1.001.

Al-Furjan, M.S.H., Moghadam, S.A., Dehini, R., Shan, L., Habibi, M. and Safarpour, H. (2021), "Vibration control of a smart shell reinforced by graphene nanoplatelets under external load: Semi-numerical and finite element modeling", *Thin Wall. Struct.*, **159**, 107242. https://doi.org/10.1016/j.tws.2020.107242

Almitani, K.H., Abdelrahman, A.A. and Eltaher, M.A. (2020), "Stability of perforated nanobeams incorporating surface energy effects", *Steel Compos. Struct.*, **35**(4), 555-566. https://doi.org/10.12989/scs.2020.35.4.555.

Ansari, R., Shahabodini, A. and Shojaei, M.F. (2016), "Nonlocal three-dimensional theory of elasticity with application to free vibration of functionally graded nanoplates on elastic foundations", *Physica E*, **76**, 70-81. https://doi.org/10.1016/j.physe.2015.09.042

Apuzzo, A., Barretta, R., Faghidian, S.A., Luciano, R. and Marotti de Sciarra, R. (2018), "Free vibrations of elastic beams by modified nonlocal strain gradient theory", *Int. J. Eng. Sci.*, **133**, 99-108. https://doi.org/10.1016/j.ijengsci.2018.09.002.

Arefi, M., Bidgoli, E.M.R. and Rabczuk, T. (2019), "Effect of various characteristics of graphene nanoplatelets on thermal buckling behavior of FGRC micro plate based on MCST", *Eur. J. Mech. A Solid.*, **77**, 103802. https://doi.org/10.1016/j.euromechsol.2019.103802.

Arefi, M., Bidgoli, M.R., Dimitri, R. and Tornabene, F. (2018), "Free vibrations of functionally graded polymer composite nanoplates reinforced with grapheme nanoplatelets", *Aerosp. Sci. Technol.*, **81**, 108-117. https://doi.org/10.1016/j.ast.2018.07.036.

Attia, M.A. and Mahmoud, F.F. (2016), "Modeling and analysis of nanobeams based on nonlocal-couple stress elasticity and surface energy theories", *Int. J. Mech. Sci.*, **105**, 126-134. https://doi.org/10.1016/j.ijmecsci.2015.11.002

Attia, M.A. (2017), "On the mechanics of functionally graded nanobeams with the account of surface elasticity", *Int. J. Eng. Sci.*, **115**, 73-101. https://doi.org/10.1016/j.ijengsci.2017.03.011.

Avcar, M. (2019), "Free vibration of imperfect sigmoid and power law functionally graded beams", *Steel Compos. Struct.*, **30**(6), 603-615. https://doi.org/10.12989/SCS.2019.30.6.603

Barretta, R. and de Sciarra, F.M. (2018), "Constitutive boundary conditions for nonlocal strain gradient elastic nano-beams", *Int. J. Eng. Sci.*, **130**, 187-198. https://doi.org/10.1016/j.ijengsci.2018.05.009.

Barretta, R., Sciarra, F.M.d. and Vaccaro, M.S. (2019), "On nonlocal mechanics of curved elastic beams", *Int. J. Eng. Sci.*, **144**, 103140. http://doi.org/10.1016/j.ijengsci.2019.1031.

Behdinan, K. and Moradi-Dastjerdi, R. (2022), "Thermal buckling resistance of a lightweight lead-free piezoelectric nanocomposite sandwich plate", *Adv. Nano Res.*, **12**(6), 593-603. https://doi.org/10.12989/ANR.2022.12.6.593

Bharath, H.S., Waddar, S., Bekinal, S.I., Jeyaraj, P. and Doddamani, M. (2020), "Effect of axial compression on dynamic response of concurrently printed sandwich", *Compos. Struct.*, 113223. https://doi.org/10.1016/j.compstruct.2020.113223.

Bochkareva, S.A. and Lekomtsev, S.V. (2022), "Natural vibrations and hydroelastic stability of laminated composite circular cylindrical shells", *Struct. Eng. Mech.*, **81**(6), 769-780. https://doi.org/10.12989/SEM.2022.81.6.769

Civalek, O. and Demir, C. (2016), "A simple mathematical model of microtubules surrounded by an elastic matrix by nonlocal finite element method", *Appl. Math. Comput.*, **289**, 335-352. https://doi.org/10.1016/j.amc.2016.05.034.

Daouadji, T.H. and Hadji, L. (2015), "Analytical solution of nonlinear cylindrical bending for functionally graded plates", *Geomech. Eng.*, **9**(5), 631-644. https://doi.org/10.12989/GAE.2015.9.5.631.

Ding, F., Ding, H., He, C., Wang, L. and Lyu, F. (2022), "Method for flexural stiffness of steel-concrete composite beams based on stiffness combination coefficients", *Comput. Concr.*, **29**(3), 127-144. https://doi.org/10.12989/CAC.2022.29.3.127

Ding, H.X., Liu, H.B., She, G.L. and Wu, F. (2023), "Wave propagation of FG-CNTRC plates in thermal environment using the high-order shear deformation plate theory", *Comput. Concr.*, **32**(2), 207-215. https://doi.org/10.12989/CAC.2023.32.2.207

Ebrahimi, F. and Dabbagh, A. (2018), "Wave dispersion characteristics of embedded graphene platelets-reinforced composite microplates", *Eur. Phys. J. Plus*, **133**, 151. https://doi.org/10.1140/epjp/i2018-11956-5.

Ebrahimi, F., Barati, M.R. and Civalek, O. (2020), "Application of Chebyshev-Ritz method for static stability and vibration analysis of nonlocal microstructure-dependent nanostructures", *Eng. Comput.*, **36**, 953-964. https://doi.org/10.1007/s00366- 019-00742-z.

Ebrahimi, F., Seyfi, A., Dabbagh, A. and Tornabene, F. (2019), "Wave dispersion characteristics of porous graphene platelet-reinforced composite shells", *Struct. Eng. Sci.*, **71**, 99-107. https://doi.org/10.12989/sem.2019.71.1.099.

Ebrahimi, F., Mohammadi, K., Barouti, M.M. and Habibi, M. (2021), "Wave propagation analysis of a spinning porous graphene nanoplatelet-reinforced nanoshell", *Waves Random Complex Med.*, **31**(6), 1655-1681. https://doi.org/10.1080/17455030.2019.1694729

Eltaher, M.A., Almalki, T.A., Ahmed, K.I.E. and Almitani, K.H. (2019), "Characterization and behaviors of single walled carbon nanotube by equivalent-continuum mechanics approach", *Adv. Nano Res.*, **7**(1), 39-49. https://doi.org/10.12989/ANR.2019.7.1.039

Eltaher, M.A. and Abdelrahman, A.A. (2020), "Bending behavior of squared cutout nanobeams incorporating surface stress effects", *Steel Compos. Struct.*, **36**(2), 143-161. https://doi.org/10.12989/scs.2020.36.2.143.

Eltaher, M.A. and Mohamed, N. (2020), "Nonlinear stability and vibration of imperfect CNTs by Doublet mechanics", *Appl. Math. Comput.*, **382**, 125311. https://doi.org/10.1016/j.amc.2020.125311

Eltaher, M.A., Khater, M.E., Park, S., Abdel-Rahman, E. and Yavuz, M. (2016), "On the static stability of nonlocal nanobeams using higher-order beam theories", *Adv. Nano Res.*, **4**(1), 51-64. https://doi.org/10.12989/ANR.2016.4.1.051

Eltaher, M.A., Omar, F.A., Abdraboh, A.M., Abdalla, W.S. and Alshorbagy, A.E. (2020), "Mechanical behaviors of piezoelectric nonlocal nanobeam with cutouts", *Smart. Struct. Syst.*, **25**(2), 219-228. https://doi.org/10.12989/sss.2020.25.2.219

Emam, S.A., Eltaher, M.A., Khater, M.E. and Abdalla, W.S. (2018), "Postbuckling and free vibration of multilayer imperfect nanobeams under a pre-stress load", *Appl. Sci. Basel*, **8**(11), 2238. https://doi.org/10.3390/app8112238

Emdadi, M., Mohammadimehr, M. and Navi, B.R. (2023), "The surface stress effects on the buckling analysis of porous micro-composite annular sandwich plate based on HSDT using Ritz method", *Comput. Concr.*, **32**(5), 439-454. https://doi.org/10.12989/CAC.2023.32.5.439

Eringen, A.C. (1998), "On differential equations of nonlocal elasticity and solutions of screw dislocation and surface waves", *J. Appl. Phys.*, **54**(9), 4703-4710. https://doi.org/10.1063/1.332803.

Esen, I., Alazwari, M.A., Almitani, K.H., Eltaher, M.A. and Abdelrahman, A. (2023), "Dynamic vibration response of functionally graded porous nanoplates in thermal and magnetic fields under moving load", *Adv. Nano Res.*, **14**(5), 475-493. https://doi.org/10.12989/ANR.2023.14.5.475

Faleh, N.M., Ahmed, R.A. and Fenjan, R.M. (2018), "On

vibrations of porous FG nanoshells", *Int. J. Eng. Sci.*, **133**, 1-14. https://doi.org/10.1016/j.ijengsci.2018.08.007.

Gao, W., Qin, Z. and Chu, F. (2020), "Wave propagation in functionally graded porous plates reinforced with grapheme platelets", *Aerosp. Sci. Technol.*, **102**, 105860. https://doi.org/10.1016/j.ast.2020.10586.

Gao, Y., Xiao, W. and Zhu, H. (2019), "Nonlinear vibration analysis of different types of functionally graded beams using nonlocal strain gradient theory and a two-step perturbation method", *Euro. Phys. J. Plus*, **134**(1), 23. https://doi.org/10.1140/epjp/i2019-12446-0

Ghayesh, M.H. and Farajpour, A. (2018), "Nonlinear mechanics of nanoscale tubes via nonlocal strain gradient theory", *Int. J. Eng. Sci.*, **129**, 84-95. https://doi.org/10.1016/j.ijengsci.2018.04.003.

Ghayesh, M.H., Farokhi, H. and Farajpour, A. (2019), "Global dynamics of fluid conveying nanotubes", *Int. J. Eng. Sci.*, **135**, 37-57. https://doi.org/10.1016/j.ijengsci.2018.11.003

Hadji, L. (2020), "Influence of the distribution shape of porosity on the bending of FGM beam using a new higher order shear deformation model", *Smart Struct. Syst.*, **26**(2), 253-262. https://doi.org/10.12989/sss.2020.26.2.253.

Hadji, L., Meziane, A. and Safa, A. (2018), "A new quasi-3D higher shear deformation theory for vibration of functionally graded carbon nanotube-reinforced composite beams resting on elastic foundation", *Struct. Eng. Mech.*, **66**(6), 771-781. https://doi.org/10.12989/sem.2018.66.6.771

Hou, S., Wu, S., Luo, J., Nasihatgozar, M. and Behshad, A. (2022), "Frequency response of elastic nanocomposite beams containing nanoparticles based on sinusoidal shear deformation beam theory", *Steel Compos. Struct.*, **45**(4), 555-562. https://doi.org/10.12989/SCS.2022.45.4.555

Hua, F., Fu, W. and Zhou, X. (2022), "Guided wave propagation in functionally graded viscoelastic polymer composite shells reinforced with graphite particles", *Wave Random Complex Med.*, 1-27. https://doi.org/10.1080/17455030.2022.2091180

Hua, F., Fu, W. and Zhou, X. (2022), "Wave propagation analysis of sandwich plates with graphite particles filled viscoelastic material core in hygrothermal environments", *Compos. Struct.*, **288**, 115380. https://doi.org/10.1016/j.compstruct.2022.115380

Hua, F., Fu, W., You, Q. and Zhou, X. (2022), "Wave dispersion characteristics of laminated carbon fiber reinforced polymer composite shells resting on viscoelastic foundations under thermal field", *Compos. Struct.*, **301**, 116225. https://doi.org/10.1016/j.compstruct.2022.116225

Hua, F., Fu, W., You, Q., Huang, Q., Abad, F. and Zhou, X. (2023), "A refined spectral element model for wave propagation in multiscale hybrid epoxy/carbon fiber/graphene platelet composite shells", *Aerosp. Sci. Technol.*, **138**, 108321. https://doi.org/10.1016/j.ast.2023.108321

Hua, F., Huang, Q., You, Q., He, W., Zhou, H. and Zhou, X. (2024), "A semi-analytical spectral element model for guided wave propagation in composite laminated conical shells", *Structures*, **65**, 106797. https://doi.org/10.1016/j.istruc.2024.106797

Huang, Y. and Wu, S. (2022), "Hybrid adaptive neuro fuzzy inference system for optimization mechanical behaviors of nanocomposite reinforced concrete", *Adv. Nano Res.*, **12**(5), 515-527. https://doi.org/10.12989/ANR.2022.12.5.515

Janghorban, M. and Tounsi, A. (2024), "Two models for wave propagation in polymer/halloysite nanotube nanocomposites: network phenomena/generalized continuum mechanics", *Wave Random Complex Med.*, 1-32. https://doi.org/10.1080/17455030.2024.2396335

Jiao, P. and Alavi, A.H. (2018), "Buckling analysis of graphene-reinforced mechanical metamaterial beams with periodic webbing patterns", *Int. J. Eng. Sci.*, **131**, 1-18. https://doi.org/10.1016/j.ijengsci.2018.06.005.

Kamarian, S. and Song, J.I. (2023), "Thermal buckling of rectangular sandwich plates with advanced hybrid SMA/CNT/graphite/epoxy composite face sheets", *Adv. Nano Res.*, **14**(3), 261-271. https://doi.org/10.12989/ANR.2023.14.3.261

Karami, B., Janghorban, M. and Rabczuk, T. (2019), "Analysis ofelastic bulk waves in functionally graded triclinic nano-platesusing a quasi-3D bi-Helmholtz nonlocal strain gradient model", *Euro. J. Mech. A Solid.*, **78**, 103822. https://doi.org/10.1016/j.euromechsol.2019.103822

Khatri, K.L. and Markad, K. (2023), "Stochastic fracture behavior analysis of infinite plates with a separate crack and a hole under tensile loading", *Comput. Concr.*, **32**(1), 99-117. https://doi.org/10.12989/CAC.2023.32.1.099

Kiani, Y. (2019), "NURBS-based thermal buckling analysis of graphene platelet reinforced composite laminated skew plates", *J. Therm. Stress.*, 1-19. https://doi.org/10.1080/01495739.2019.1673687.

Kim, D.Y., Sim, C.H., Park, J.S., Yoo, J.T., Yoon, Y.H. and Lee, K. (2023), "Numerical vibration correlation technique analyses for composite cylinder under compression and internal pressure", *Struct. Eng. Mech.*, **87**(5), 419-429. https://doi.org/10.12989/SEM.2023.87.5.419

Li, C., Han, Q., Wang, Z. and Wu, X. (2020), "Analysis of wave propagation in functionally graded piezoelectric composite plates reinforced with graphene platelets", *Appl. Math. Model.*, **81**, 487-505. https://doi.org/10.1016/j.apm.2020.01.01.

Lim, C.W., Zhang, G. and Reddy, J.N. (2015), "A higher-order nonlocal elasticity and strain gradient theory and its applications in wave propagation", *J. Mech. Phys. Solids*, **78**, 298-313. https://doi.org/10.1016/j.jmps.2015.02.00.

Liu, H., Wu, H. and Lyu, Z. (2020), "Nonlinear resonance of FG multilayer beam-type nanocomposites: Effects of grapheme nanoplatelet-reinforcement and geometric imperfection", *Aerosp. Sci. Technol.*, **98**, 105702. https://doi.org/10.1016/j.ast.2020.105702.

Lu, L., Guo, X. and Zhao, J. (2018), "On the mechanics of Kirchhoff and Mindlin plates incorporating surface energy", *Int. J. Eng. Sci.*, **124**, 24-40. https://doi.org/10.1016/j.ijengsci.2017.11.020.

Madenci, E. (2019), "A refined functional and mixed formulation to static analyses of fgm beams", *Struct. Eng. Mech.*, **69**(4), 427-437. https://doi.org/10.12989/sem.2019.69.4.427.

Madenci, E. and Özütok, A. (2020), "Variational approximate for high order bending analysis of laminated composite plates", *Struct. Eng. Mech.*, **73**(1), 97-108. https://doi.org/10.12989/sem.2020.73.1.097.

Madenci, E., Gulcu, S. and Draiche, K. (2024), "Analytical nonlocal elasticity solution and ANN approximate for free vibration response of layered carbon nanotube reinforced composite beams", *Adv. Nano Res.*, **16**(3), 251-263. https://doi.org/10.12989/ANR.2024.16.3.251

Malikan, M., Krasheninnikov, M. and Eremeyev, V.A. (2020), "Torsional stability capacity of a nano-composite shell based on a nonlocal strain gradient shell model under a three-dimensional magnetic field", *Int. J. Eng. Sci.*, **148**, UNSP 103234. https://doi.org/10.1016/j.ijengsci.2019.10321

Malikan, M., Tornabene, F. and Dimitri, R. (2018), "Nonlocal three-dimensional theory of elasticity for buckling behavior of functionally graded porous nanoplates using volume integrals", *Mater. Res. Exp.*, **5**(9), 095006. https://doi.org/10.1088/2053-1591/aad4c3

Man, Y. (2022), "On the dynamic stability of a composite beam via modified high-order theory", *Comput. Concr.*, **30**(2), 151-164. https://doi.org/10.12989/CAC.2022.30.2.151

Mehar, K. and Panda, S.K. (2019), "Multiscale modeling approach for thermal buckling analysis of nanocomposite curved structure", *Adv. Nano Res.*, **7**(3), 181-190.

https://doi.org/10.12989/ANR.2019.7.3.181.

Mehar, K., Panda, S.K., Yuvarajan, D., Gautam, C. (2019), "Numerical buckling analysis of graded CNT-reinforced composite sandwich shell structure under thermal loading", *Compos. Struct.*, S0263822318344763. https://doi.org/10.1016/j.compstruct.2019.03.002.

Merzoug, M., Bourada, M., Sekkal, M., Ali Chaibdra, A., Belmokhtar, C., Benyoucef, S. and Benachour, A. (2020), "2D and quasi 3D computational models for thermoelastic bending of FG beams on variable elastic foundation: Effect of the micromechanical models", *Geomech. Eng.*, **22**(4), 361-374. https://doi.org/10.12989/gae.2020.22.4.361.

Mohamed, N., Mohamed, S.A., Abdelrhmaan, A.A. and Eltaher, M.A. (2023), "Nonlinear stability of bio-inspired composite beams with higher order shear theory", *Steel Compos. Struct.*, **46**(6), 759-772. https://doi.org/10.12989/SCS.2023.46.6.759

Moradi, S. and Mansouri, M.H. (2012), "Thermal buckling analysis of shear deformable laminated orthotropic plates by differential quadrature", *Steel Compos. Struct.*, **12**(2), 129-147. https://doi.org/10.12989/scs.2012.12.2.129.

Panda, S.K., Singh, B.N. (2013), "Nonlinear finite element analysis of thermal post-buckling vibration of laminated composite shell panel embedded with SMA fibre", *Aerosp. Sci. Technol.*, **29**(1), 47-57. https://doi.org/10.1016/j.ast.2013.01.007.

Pinnola, F.P., Faghidian, S.A., Barretta, R. and Marotti de Sciarra, F. (2020), "Variationally consistent dynamics of nonlocal gradient elastic beams", *Int. J. Eng. Sci.*, **149**, 103220. https://doi.org/10.1016/j.ijengsci.2020.103220

Rachedi, M.A., Benyoucef, S., Bouhadra, A., Bachir Bouiadjra, R., Sekkal, M., Benachour, A. (2020), "Impact of the homogenization models on the thermoelastic response of FG plates on variable elastic foundation", *Geomech. Eng.*, **22**(1), 65-80. https://doi.org/10.12989/gae.2020.22.1.065.

Sahmani, S.S., Aghdam, M.M. and Rabczuk, T. (2018), "Nonlocal strain gradient plate model for nonlinear large-amplitude vibrations of functionally graded porous micro/nano-plates reinforced with GPLs", *Compos. Struct.*, **198**, 51-62. https://doi.org/10.1016/j.compstruct.2018.05.031.

Sahoo, S., Parida, S.P. and Jena, P.C. (2023), "Dynamic response of a laminated hybrid composite cantilever beam with multiple cracks & moving mass", *Struct. Eng. Mech.*, **87**(6), 529-540. https://doi.org/10.12989/SEM.2023.87.6.529

Sahu, P., Sharma, N. and Panda, S.K. (2020), "Numerical prediction and experimental validation of free vibration responses of hybrid composite (glass/carbon/kevlar) curved panel structure", *Compos. Struct.*, 112073. https://doi.org/10.1016/j.compstruct.2020.112073.

Selmi, A. (2020), "Exact solution for nonlinear vibration of clamped-clamped functionally graded buckled beam", *Smart Struct. Syst.*, **26**(3), 361-371. https://doi.org/10.12989/SSS.2020.26.3.361.

Shanab, R.A., Mohamed, N.A., Eltaher, M.A. and Abdelrahman, A.A. (2023), "Dynamic characteristics of viscoelastic nanobeams including cutouts", *Adv. Nano Res.*, **14**(1), 45-65. https://doi.org/10.12989/ANR.2023.14.1.045

She, G.L. (2020), "Wave propagation of FG polymer composite nanoplates reinforced with GNPs", *Steel Compos. Struct*, **37**(1), 27-35. https://doi.org/10.12989/scs.2020.37.1.027

She, G.L., Liu, H.B. and Karami, B. (2020), "On resonance behavior of porous FG curved nanobeams", *Steel Compos. Struct.*, **36**(2), 179-186. https://doi.org/10.12989/scs.2020.36.2.179.

Singh, V.K. and Panda, S.K. (2014), "Nonlinear free vibration analysis of single/doubly curved composite shallow shell panels", *Thin Wall. Struct.*, **85**, 341-349. https://doi.org/10.1016/j.tws.2014.09.003.

Sobhy, M. (2015), "A comprehensive study on FGM nanoplates embedded in an elastic medium", *Compos. Struct.*, **134**, 966-980. https://doi.org/10.1016/j.compstruct.2015.08.102

Song, M., Yang, J. and Kitipornchai, S. (2018), "Bending and buckling analyses of functionally graded polymer composite plates reinforced with graphene nanoplatelets", *Compos. Part B Eng.*, **134**, 106-113. https://doi.org/10.1016/j.compositesb.2017.09.043

Taherifar, R., Mahmoudi, M., Nasr Esfahani, M.H., Khuzani, N.A., Esfahani, S.N. and Chinaei, F. (2019), "Buckling analysis of concrete plates reinforced by piezoelectric nanoparticles", *Comput. Concr.*, **23**(4), 295-301. https://doi.org/10.12989/cac.2019.23.4.295

Tayebi, M.S., Salami, S.J. and Tavakolian, M. (2023), "Free vibration analysis of FG composite plates reinforced with GPLs in thermal environment using full layerwise FEM", *Struct. Eng. Mech.*, **85**(4), 445-459. https://doi.org/10.12989/SEM.2023.85.4.445

Thai, H.T., Park, T. and Choi, D.H. (2013), "An efficient shear deformation theory for vibration of functionally graded plates", *Arch. Appl. Mech.*, **83**, 137-149. https://doi.org/10.1007/s00419-012-0642-4

Timesli, A. (2020), "Prediction of the critical buckling load of SWCNT reinforced concrete cylindrical shell embedded in an elastic foundation", *Comput. Concr.*, **26**(1), 53-62. https://doi.org/10.12989/CAC.2020.26.1.053.

Tounsi, A., Tahir, S.I., Mudhaffar, I.M., Al-Osta, M.A. and Chikh, A. (2024), "On the wave propagation characteristics of functionally graded porous shells", *HCMCOU J. Sci. Adv. Comput. Struct.*, **14**(1).

Tran, T.T., Tran, V.K., Le, P.B., Phung, V.M., Do, V.T. and Nguyen, H.N. (2020). "Forced vibration analysis of laminated composite shells reinforced with graphene nanoplatelets using finite element method", *Adv. Civil Eng.*, 1471037. https://doi.org/10.1155/2020/1471037

Turan, F. (2023), "Stability of the porous orthotropic laminated composite plates via the hyperbolic shear deformation theory", *Steel Compos. Struct.*, **48**(2), 145-161. https://doi.org/10.12989/SCS.2023.48.2.145

Turini, T.T. and Calenzani, A.F.G. (2022), "Analytical study of composite steel-concrete beams with external prestressing", *Struct. Eng. Mech.*, **82**(5), 595-609. https://doi.org/10.12989/SEM.2022.82.5.595

Uzun, B. and Civalek, O. (2019), "Nonlocal FEM formulation for vibration analysis of nanowires on elastic matrix with different materials", *Math. Comput. Appl.*, **24**(2), 38. https://doi.org/doi:10.3390/mca2402003

Vantadori, S., Luciano, R., Scorza, D. and Darban, H. (2022), "Fracture analysis of nanobeams based on the stress-driven non-local theory of elasticity", *Mech. Adv. Mater. Struct.*, **29**(14), 1967-1976. https://doi.org/10.1080/15376494.2020.1846231

Vinyas, M. (2020), "On frequency response of porous functionally graded magneto-electro-elastic circular and annular plates with different electro-magnetic conditions using HSDT", *Compos. Struct.*, **240**, 112044. https://doi.org/10.1016/j.compstruct.2020.112044.

Wang, X., Guo, X., Babaei, M., Fili, R. and Farahani, H. (2023), "Natural frequency analysis of joined conical-cylindrical-conical shells made of graphene platelet reinforced composite resting on Winkler elastic foundation", *Adv. Nano Res.*, **15**(4), 367-384. https://doi.org/10.12989/ANR.2023.15.4.367

Wu, X. (2023), "Nonlinear finite element vibration analysis of functionally graded nanocomposite spherical shells reinforced with graphene platelets", *Adv. Nano Res.*, **15**(2), 141-153. https://doi.org/10.12989/ANR.2023.15.2.141

Xia, J., Jafari, G.S. and Ghoroughi, F. (2024), "New method environment for art design of nanocomposite brick facade of the building", *Steel Compos. Struct.*, **51**(5), 499-507.

https://doi.org/10.12989/SCS.2024.51.5.499
Xu, G. and Ming, F. (2023), "On dynamic response and economic of sinusoidal porous laminated nanocomposite beams using numerical method", *Steel Compos. Struct.*, **49**(3), 349-359. https://doi.org/10.12989/SCS.2023.49.3.349
Yaghoobi, H. and Taheri, F. (2020), "Analytical solution and statistical analysis of buckling capacity of sandwich plates with uniform and non-uniform porous core reinforced with graphene nanoplatelets", *Compos. Struct.*, **252**, 112700. https://doi.org/10.1016/j.compstruct.2020.112700
Yahea, H.T. and Majeed, W.I. (2021), "Free vibration of laminated composite plates in thermal environment using a simple four variable plate theory", *Compos. Mater. Eng.*, **3**(3), 179-199. https://doi.org/10.12989/cme.2021.3.3.179.
Yang, Z., Liu, A., Yang, J., Fu, J. and Yang, B. (2020), "Dynamic buckling of functionally graded graphene nanoplatelets reinforced composite shallow arches under a step central point load", *J. Sound Vib.*, **465**, 115019. https://doi.org/10.1016/j.jsv.2019.11501
Yang, Z., Wu, D., Yang, J., Lai, S.K., Lv, J., Liu, A. and Fu, J. (2021), "Dynamic buckling of rotationally restrained FG porous arches reinforced with graphene nanoplatelets under a uniform step load", *Thin Wall. Struct.*, **166**, 108103. https://doi.org/10.1016/j.tws.2021.108103
Yaylaci, E.U., Yaylaci, M., Ozdemir, M.E., Terzi, M. and Ozturk, S. (2023), "Analyzing the mechano-bactericidal effect of nano-patterned surfaces by finite element method and verification with artificial neural networks", *Adv. Nano Res.*, **15**(2), 165-174. https://doi.org/10.12989/ANR.2023.15.2.165
Zhao, T., Ma, Y., Zhou, J. and Fu, Y. (2021). "Wave propagation in rotating functionally graded microbeams reinforced by graphene nanoplatelets", *Molecules*, **26**(17), 5150. https://doi.org/10.3390/molecules26175150